

# Reverse engineering in many-body quantum physics: What many-body system corresponds to an effective single-particle equation?

J. P. Coe<sup>1,2,\*</sup>, K. Capelle<sup>3,4</sup>, and I. D'Amico<sup>1†</sup>

<sup>1</sup> *Department of Physics, University of York, York YO10 5DD, United Kingdom.*

<sup>2</sup> *Department of Mathematics, University of York, York YO10 5DD, United Kingdom.*

<sup>3</sup> *Departamento de Física e Informática, Instituto de Física de São Carlos, Universidade de São Paulo, Caixa Postal 369, 13560-970 São Carlos, SP, Brazil.*

<sup>4</sup> *Theoretische Physik, Freie Universität Berlin, D-14195 Berlin, Germany.*

(Dated: February 26, 2019)

The mapping, exact or approximate, of a many-body problem onto an effective single-body problem is one of the most widely used conceptual and computational tools of physics. Here, we propose and investigate the inverse map of effective approximate single-particle equations onto the corresponding many-particle system. This approach allows us to understand which interacting system a given single-particle approximation is actually describing, and how far this is from the original physical many-body system. We illustrate the resulting reverse engineering process by means of the Kohn-Sham equations of density-functional theory. In this application, our procedure sheds light on the non-locality of the density-potential mapping of DFT, and on the self-interaction error inherent in approximate density functionals.

PACS numbers: 71.10.-w, 31.15.eg, 71.15.Mb

One of the most widely used and successful approaches to many-particle physics is to map the many-body problem onto an effective single-body problem. Innumerable concepts and methods of theoretical physics derive from this general idea. The mean-field approximation, one of the most widely used approximation schemes in all fields of physics, is of this type, as well as the (in principle exact) mapping onto Kohn-Sham (KS) equations, used in density-functional theory (DFT). Here we introduce the concept of *reverse engineering of single-particle equations*,<sup>1</sup> as a tool for discovering for which many-body system a given single-particle approximation becomes exact. The idea is developed below in the framework of DFT, but the concept is completely general, and can be extended to other single-particle methods.

DFT<sup>2-4</sup> in the Kohn-Sham formulation<sup>5</sup> is a tool for calculating properties of many-body systems by means of a one-to-one mapping between the interacting system and a fictitious non-interacting one, with the same ground-state density  $n(\mathbf{r})$ . All ground-state properties can in principle be expressed as functionals of this density. The success of DFT depends on the quality of the approximation to the exchange-correlation (xc) energy functional  $E_{xc}[n]$ , which enters the KS equations through its functional derivative, the xc potential  $v_{xc}(\mathbf{r})$ .  $E_{xc}$  stems from the interactions in the original many-body system, and its functional form for Coulomb interacting systems, such as electrons in atoms, molecules, nanostructures and solids, is unknown. In order to construct viable approximations, a great deal of work has therefore been devoted to the derivation of exact properties of the exchange-correlation functional and potential.<sup>6,7</sup>

Traditionally, the functional is made exact in certain limits (such as uniform densities in the local-density approximation [LDA]) or for certain systems (such as the training sets employed in the construction of empirical functionals). For systems away from these limits or the training set, the functional is approximate. The performance of a functional is then judged by how close the density, and the observables calcu-

lated from it, are to that of the many-body system under study. The idea of reverse engineering suggests a different mode of analysis, namely to ask: for what system does a given approximation become exact? This question can be interpreted in two ways, one very common, the other being proposed here. To exemplify both, consider the LDA. By construction, the LDA becomes exact for uniform densities. But in practice we rarely apply density functionals to uniform systems. Instead, we apply DFT to realistic inhomogeneous many-body systems, for which the LDA density is  $\mathbf{r}$ -dependent and approximate. The question we ask is: for which alternative many-body system is this approximate density the exact ground-state density? In this context, we call this alternative many-body system the interacting-LDA (i-LDA) system.<sup>8</sup> Reverse engineering of DFT allows us to view the quality of an approximate  $v_{xc}$  for a given system in another light, as we can now ask: how close is the corresponding i-system external potential to the true external potential? Which artificial features is the chosen approximation building into the system?

More generally, the approximate density could be the result of experiments, of density-functional calculations with some approximate  $E_{xc}$ , or of some other computational approach, such as Monte Carlo simulations. In all these cases, we can compare the true many-body system (for which  $n(\mathbf{r})$  is approximate) to the alternative many-body system (for which  $n(\mathbf{r})$  is exact). As in other parts of science, reverse engineering enables one to understand the functionality and structure of the engineered device on a different level, and opens up new pathways for improvement.

To illustrate the basic idea, we start from the LDA densities of the Helium atom and of Hooke's atom, and invert the many-body Schrödinger equation to construct that external potential for which the LDA densities are exact ground-state densities. Comparison to the true external potentials of the Helium atom ( $\sim 1/r$ ) and Hooke's atom ( $\sim r^2$ ) reveals the errors inherent in the approximate density and functional. Earlier inversion schemes in DFT were used to find the  $v_{xc}(\mathbf{r})$  that reproduces

a given exact density, by inverting the single-particle Kohn-Sham equations.<sup>9-15</sup> This approach provides information on the exact  $v_{xc}$ . The reverse engineering procedure, by contrast, aims at reproducing a given approximate density by inverting the many-body Schrödinger equation, providing information on the approximate  $v_{xc}$ . Inversion of the many-body equation is a much harder task, which up to now had only been attempted for a one-dimensional model system within the adiabatic approximation to time-dependent DFT.<sup>16</sup> To achieve this, we developed inversion schemes that are substantially more accurate than previous ones (see discussion below).

We consider the N-body Hamiltonian  $H = \hat{T} + \hat{V}_{ee} + \hat{V}_{ext}$ , where  $\hat{T}$  is the kinetic energy operator,  $\hat{V}_{ee}$  is the electron-electron interaction and  $\hat{V}_{ext} = \sum_{i=1}^N v_{ext}(\mathbf{r}_i)$ , is the external potential. By multiplying the Schrödinger equation  $\hat{H}\Psi = E\Psi$  from the left by  $\Psi^*$  and integrating over all but one of the coordinates we obtain

$$\int \Psi^*(\mathbf{r}_1 \dots \mathbf{r}_N) (\hat{T} + \hat{V}_{ee} + \hat{V}_{ext}) \Psi(\mathbf{r}_1 \dots \mathbf{r}_N) d^3r_2 \dots d^3r_N = E \frac{n(\mathbf{r}_1)}{N}. \quad (1)$$

From this we find, for the term concerning the external potential,

$$\int \Psi^* \sum_{i=1}^N v_{ext}(\mathbf{r}_i) \Psi d^3r_2 \dots d^3r_N = v_{ext}(\mathbf{r}_1) \frac{n(\mathbf{r}_1)}{N} + (N-1) \int \Psi^* v_{ext}(\mathbf{r}_2) \Psi d^3r_2 \dots d^3r_N \quad (2)$$

$$= v_{ext}(\mathbf{r}_1) \frac{n(\mathbf{r}_1)}{N} + \frac{2}{N} \int \gamma(\mathbf{r}_1, \mathbf{r}_2; \mathbf{r}_1, \mathbf{r}_2) v_{ext}(\mathbf{r}_2) d^3r_2, \quad (3)$$

where  $\gamma(\mathbf{r}_1, \mathbf{r}_2; \mathbf{r}_1, \mathbf{r}_2) = \frac{N(N-1)}{2} \int \Psi^* \Psi d^3r_3 \dots d^3r_N$ .

We combine these results to obtain an iterative relation for the external potential  $v_{ext}(\mathbf{r}_1)$  that reproduces the target density  $n^{\text{target}}(\mathbf{r}_1)$ ,

$$\begin{aligned} v_{ext}^{i+1}(\mathbf{r}_1) &= \frac{1}{n_i(\mathbf{r}_1)} [E_i n^{\text{target}}(\mathbf{r}_1) \\ &- N \int \Psi_i^* (\hat{T} + \hat{V}_{ee}) \Psi_i d^3r_2 \dots d^3r_N \\ &- 2 \int \gamma_i(\mathbf{r}_1, \mathbf{r}_2; \mathbf{r}_1, \mathbf{r}_2) v_{ext}^i(\mathbf{r}_2) d^3r_2]. \end{aligned} \quad (4)$$

To avoid having to calculate the integrals, we use the identity

$$\begin{aligned} n_i(\mathbf{r}_1) v_{ext}^i(\mathbf{r}_1) - E_i n_i(\mathbf{r}_1) &= \\ &- N \int \Psi_i^* (\hat{T} + \hat{V}_{ee}) \Psi_i d^3r_2 \dots d^3r_N \\ &- 2 \int \gamma_i(\mathbf{r}_1, \mathbf{r}_2; \mathbf{r}_1, \mathbf{r}_2) v_{ext}^i(\mathbf{r}_2) d^3r_2, \end{aligned} \quad (5)$$

and obtain the simple iterative relation

$$v_{ext}^{i+1}(\mathbf{r}_1) = \frac{1}{n_i(\mathbf{r}_1)} E_i [n^{\text{target}}(\mathbf{r}_1) - n_i(\mathbf{r}_1)] + v_{ext}^i(\mathbf{r}_1), \quad (6)$$

which is to be iterated with the Schrödinger equation  $(\hat{T} + \hat{V}_{ee} + \hat{V}_{ext}^i) \Psi_i = E_i \Psi_i$ . At convergence,  $n_i(\mathbf{r}_1) \equiv n^{\text{target}}(\mathbf{r}_1)$ , and  $v_{ext}^{i+1}(\mathbf{r}_1) \equiv v_{ext}^i(\mathbf{r}_1)$  is the external potential that reproduces this density via the many-body Schrödinger equation.

We note that if  $n_i(\mathbf{r}_1)$  is larger (smaller) than  $n^{\text{target}}(\mathbf{r}_1)$  then the potential must increase (decrease) at this point to bring  $n_{i+1}(\mathbf{r}_1)$  closer to  $n^{\text{target}}(\mathbf{r}_1)$ . Therefore, iteration of Eq. (6) is expected to converge if  $E_i < 0$ . If  $E_i > 0$ , we replace Eq. (6) by

$$v_{ext}^{i+1}(\mathbf{r}_1) = \frac{1}{n_i(\mathbf{r}_1)} E_i [n_i(\mathbf{r}_1) - n^{\text{target}}(\mathbf{r}_1)] + v_{ext}^i(\mathbf{r}_1). \quad (7)$$

Scheme (6) converges relatively easily for the Helium atom (where  $E < 0$ ) and scheme (7) for Hooke's atom (where  $E > 0$ ). We aid convergence in both cases by mixing  $v_{ext}^{i+1}$  with 80% of  $v_{ext}^i$ , and iterate until the relative error  $\int d^3r |n_i(\mathbf{r}) - n^{\text{target}}(\mathbf{r})| / \int d^3r n^{\text{target}}(\mathbf{r})$  has reached a desired level.

At convergence, we obtain that external potential whose many-body ground state has the same density as was predicted by the approximate density functional for the true external potential. We check this property by independently solving the many-body Schrödinger equation with the converged alternative external potential, using a larger basis set than that used in the iterations. This additional consistency procedure allows our inversion scheme to be precise even in regions of space where the density is just  $10^{-7}$  a.u. (Helium) and  $10^{-12}$  a.u. (Hooke's atom), i.e. orders of magnitudes smaller than previous inversion schemes, which, according to Ref. 16 attain an accuracy of up to  $10^{-2}$  a.u.

We now illustrate both inversion schemes, and the additional consistency check, by applying our procedure to the Helium atom and Hooke's atom, generating the approximate (target) density from the LDA. For two electrons in a spherically symmetric potential the ground state can only be a function of the distance of each electron from the origin and the angle between the electron vectors. Hence we employ the basis

$$\phi_{ijl} = R_i(r_1) R_j(r_2) \sqrt{2l+1} P_l(\cos(\theta)) / (4\pi). \quad (8)$$

For Hooke's atom  $R_i(r) = Q_i(r) e^{-\alpha r^2}$  is a harmonic oscillator-like wave-function while for the Helium atom it is a hydrogen-like wave-function  $R_i(r) = Q_i(r) e^{-\alpha r}$ . The  $Q_i(r)$  are polynomials of degree  $i$  created via the Gram-Schmidt procedure such that the  $R_i$  are orthonormal.

Hooke's atom is an interacting system of two electrons in the harmonic confining potential  $v_{ext} = \omega r^2/2$ . We use the LDA in the parametrization of Perdew and Wang<sup>18</sup> for  $v_{xc}$ , and solve the KS equations for  $\hbar\omega = 0.0365$  Hartree. For comparison we also calculate the exact density from the exact interacting wave function using the method of Taut.<sup>19</sup> We then apply Eq. (7) to find the external potential of the interacting system that reproduces the LDA density, i.e. the i-LDA system.<sup>8</sup>

In practice, an external potential found with a basis of e.g.  $6^3$  functions may not reproduce the LDA density when we counter-check the scheme by solving the many-body Schrödinger equation of the i-LDA system using a larger basis

of size e.g.  $7^3$ . Hence, we repeat the procedure with increasing basis size until we find an external potential that reproduces the LDA density even with a larger basis.

In Fig. 1 (a) the exact and LDA densities are plotted. The LDA and i-LDA densities are indistinguishable, but the difference between the LDA and exact densities is large, and consequently the potentials of the true and the i-LDA system are rather different. Fig. 1(c) shows a substantial difference between the i-LDA potential and the true external potential at large  $r$ , where the i-LDA potential grows more rapidly than the true potential. The LDA density is very different from the true density in this region (Fig. 1 (a) inset), with a relative error  $(n(r) - n^{\text{LDA}}(r))/n^{\text{LDA}} \sim 60\%$  for  $r = 28$ .<sup>20</sup> By contrast, near the origin the i-LDA potential is slightly weaker than the true one. In between the two limiting regions, the i-LDA potential and the true external potential cross various times. These crossings manifest themselves in a complex way in the behavior of the corresponding densities: Fig. 1 shows that a crossing in the potentials around  $r = 8$  (Fig. 1 (c) inset) corresponds to a crossing in the densities (Fig. 1 (b)), whereas the crossings at  $r \sim 2$  and  $r \sim 25$  are not accompanied by a crossing in the densities.

Next we consider the Helium atom, for which we use the iterative scheme of Eq. (6) to calculate the i-LDA external potential. Here a basis of  $7^3$  functions is required to find the external potential that satisfies our consistency check, i.e. reproduces the density when solving the Schrödinger equation with a larger basis ( $8^3$  functions).

As Fig. 2 shows, the LDA reproduces relatively well the exact radial probability density, but an underestimate at small  $r$  and overestimate at large  $r$  is evident. A closer view of large  $r$  (inset of Fig. 2(b)) shows that there is a larger discrepancy (49% on the range  $4 \leq r/a_0 \leq 5.5$  compared to 3.68% overall) between the LDA density and the exact density here. However we still find that the i-LDA system density is almost indistinguishable from the LDA density on this scale (0.78% error) and its overall error at 0.037% is comparable to that of 0.0063% which we achieved for Hooke's atom. In Fig. 2(c) we again note that the external potential of the i-LDA system is substantially different from the true one for large values of  $r$ , where it is weaker than the true potential, causing the LDA density to be spread out slightly more than the exact one. We also observe a crossing of both potentials and densities for  $r \sim 1.2$  (Fig. 2(b)) where the radial probability density is high.

Both Hooke's and Helium atom thus exhibit a relationship between crossings in densities and crossings in potentials, but this relation is simple only in regions where the radial probability density is high. In these regions, the density at  $r$  has a strong and *local* effect on the potential, but their relationship in general is *non-local*. This non-locality implies that crossings in the potentials for low values of the radial probability density do not necessarily correspond to crossings in the densities: the LDA density can be higher than the exact density in regions where the i-LDA external potential is more repulsive than the true external potential. This dramatically highlights the non-local nature of the density-potential mapping in DFT.

Apart from the non-locality of the density-potential map-

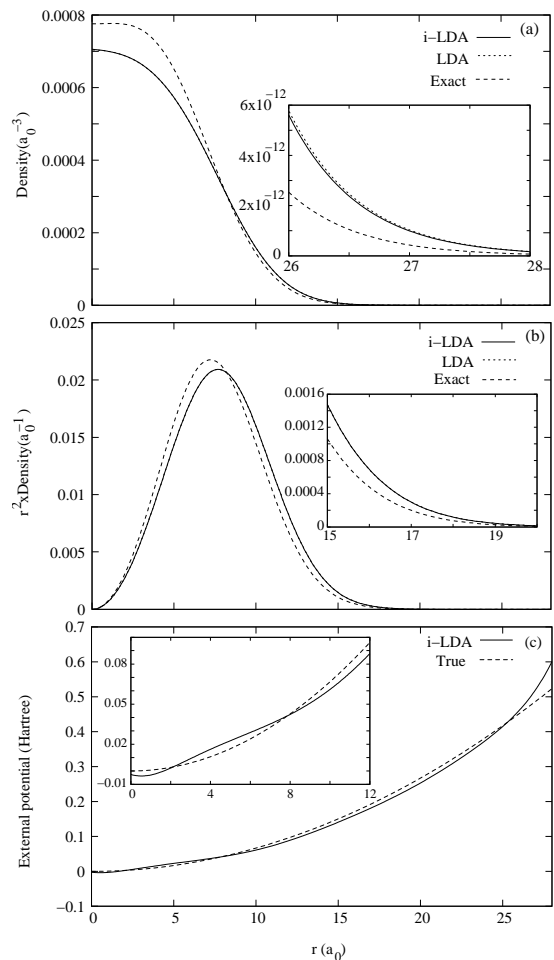


FIG. 1: Hooke's atom:  $\hbar\omega = 0.0365$  Hartree, basis size:  $8^3$  functions (counter-checked with a  $9^3$  basis set, see text). (a) Comparison of LDA, exact and i-LDA densities. Inset: Zoom of the LDA and i-LDA densities at large  $r$ . (b) Comparison of LDA, exact and the i-LDA radial probability densities. Inset: Zoom of the tail of the density. (c) Comparison of the true external potential and the i-LDA external potential. Inset: Zoom of the potentials close to the origin.

ping that is already apparent on the level of the LDA, the other main feature common to both systems is the substantial difference between the i-LDA and exact external potential at large  $r$ . For Hooke's atom in particular, the i-LDA potential diverges to infinity even faster than the exact potential.<sup>21</sup> We explain this as a consequence of the erroneous asymptotic decay of the LDA exchange-correlation potential (exponential rather than  $1/r$ ), which itself is a consequence of the single-electron self-interaction error inherent in the LDA. Due to this error, the LDA  $xc$  potential is too weak in the asymptotic region, so that the i-LDA potential and exact potentials strongly differ in this region and, at least for the Hooke's atom,<sup>22</sup> the i-LDA potential becomes much too confining at very large  $r$ 's. However in this region  $n^{\text{LDA}}(r)$  is still larger than the exact density. Common to both systems is the drop in the i-LDA external potential after the crossing at intermediate  $r$ 's, this crossing is common to both potentials and densities. We speculate that this feature is caused by a less investigated

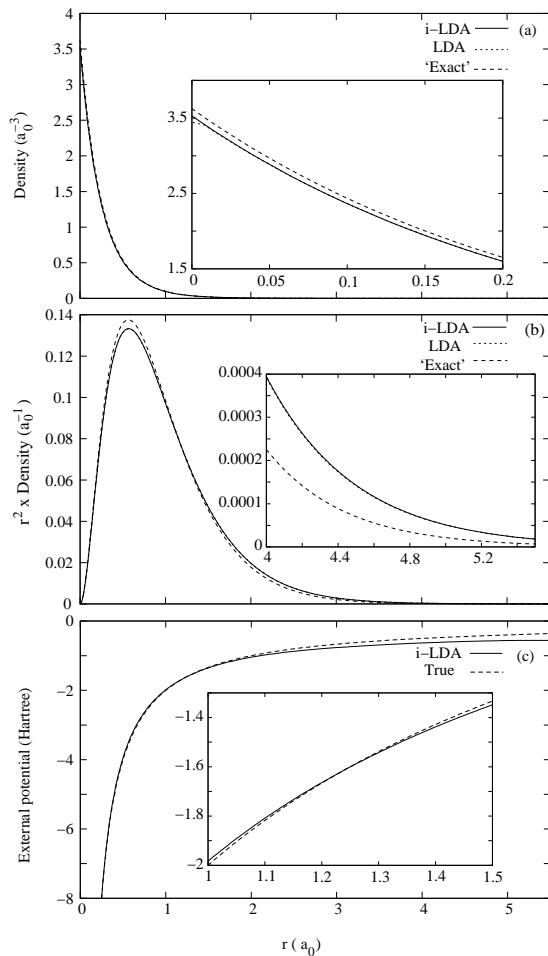


FIG. 2: Helium atom: (a) Comparison of LDA, exact and i-LDA densities. Inset: zoom of the densities close to the origin. (b) Comparison of LDA, exact and the i-LDA radial probability densities. Inset: Zoom of the tail of the density. (c) Comparison of the true external potential and the i-LDA external potential.

consequence of self-interaction, causing the electron density to spread out more at smaller  $r$  in an attempt to minimize the self-Coulomb energy. As this starts to occur before the asymptotic region is reached, it involves many electrons, and can thus be interpreted as a consequence of the many-electron self-interaction error, which has recently taken center stage in density-functional development.<sup>23,24</sup>

These considerations illustrate the use of comparing the actual many-body system under study with the alternative one for which a given single-body approximation becomes exact. To illustrate this idea we have developed, within one particular many-body theory, DFT, two iterative schemes for inverting the many-body Schrödinger equation. Previous inversion schemes within DFT either were concerned with inverting the much simpler single-particle KS equation, or directed at a one-dimensional model many-body system. Our schemes attain orders of magnitude higher accuracy than previous schemes and are applicable to real three-dimensional systems.

Building on this technical advance, we have introduced the concept of *reverse engineering* in DFT and, more generally, in all many-body methods that introduce an effective single-body potential. This approach allows one to judge the performance and failures of, *e.g.*, an approximate density functional or single-particle equation, by comparing two external potentials, thus revealing a wealth of information on properties such as, *e.g.*, self-interaction errors and non-locality, in a physically transparent way. Another application of quantum reverse engineering is to design that external potential that reproduces a desired density distribution in a given spatially inhomogeneous many-body system, which is an exciting prospect for the design of nanostructured devices.

JPC was supported by EPSRC-GB. KC was supported by FAPESP and CNPq. IDA and JPC acknowledge support from the Department of Physics of the University of York and the kind hospitality of IFSC-USP (BR).

\* Electronic address: jpc503@york.ac.uk

† Electronic address: ida500@york.ac.uk

<sup>1</sup> The usual challenge in engineering is to design a device with a given functionality in mind. Reverse engineering refers to the inverse process where one tries to understand, and then improve, the construction and operation of a given device whose functionality and design principles are *a priori* unknown.

<sup>2</sup> W. Kohn, *Rev. Mod. Phys.* **71**, 1253 (1999).

<sup>3</sup> R. M. Dreizler and E. K. U. Gross, *Density Functional Theory* (Springer-Verlag, Berlin, 1990).

<sup>4</sup> R. G. Parr and W. Yang, *Density-Functional Theory of Atoms and Molecules* (Oxford University Press, New York, 1989).

<sup>5</sup> W. Kohn and L. J. Sham, *Phys. Rev.* **140**, 1133 (1965).

<sup>6</sup> M. Levy and J. P. Perdew, *Int. J. Quantum Chem.* **49**, 539 (1994)

<sup>7</sup> J. P. Perdew, A. Ruzsinszky, J. Tao, V. N. Staroverov, G. E. Scuseria and G. I. Csonka, *J. Chem. Phys.* **123**, 062201 (2005).

<sup>8</sup> J. P. Coe, A. Sudbery, I. D'Amico, *Phys. Rev. B* **77**, 205122 (2008).

<sup>9</sup> C. -O. Almbladh and A. C. Pedroza, *Phys. Rev. A* **29**, 2322

(1984).

<sup>10</sup> N. H. March and R. F. Nalewajski, *Phys. Rev. A* **35**, 525 (1987).

<sup>11</sup> Y. Wang and R. G. Parr, *Phys. Rev. A* **47**, R1591 (1993).

<sup>12</sup> R. van Leeuwen and E. J. Baerends, *Phys. Rev. A* **49**, 2421 (1994).

<sup>13</sup> Q. Zhao, R. C. Morrison, and R. G. Parr, *Phys. Rev. A* **50**, 2138 (1994).

<sup>14</sup> Q. Zhao and R. G. Parr, *J. Chem. Phys.* **98** 1, 543, (1993).

<sup>15</sup> C. Filippi, C. J. Umrigar, and M. Taut, *J. Chem. Phys.* **100** 2, 1290, (1994).

<sup>16</sup> M. Thiele, E. K. U. Gross, and S. Kummel, *PRL* **100**, 153004 (2008).

<sup>17</sup> P. Hohenberg and W. Kohn, *Phys. Rev.* **136**, 864 (1964).

<sup>18</sup> J. P. Perdew and Y. Wang, *Phys. Rev. B* **45**, 13244 (1992).

<sup>19</sup> M. Taut, *Phys. Rev. A* **48**, 3561 (1993).

<sup>20</sup> We note that for the same  $r$ , our inversion procedure produces a much better match of  $(n^{i-LDA}(r) - n^{LDA}(r))/n^{LDA}(r) \sim 3\%$ .

<sup>21</sup> Though details as the exact crossing point may slightly differ depending on the behavior of the convergency of the i-LDA to the LDA density in that regions (where both densities are  $\sim 10^{-11}$

a.u.), the crossing of the potentials at large  $r$ 's is, in all our tests, a robust feature of Hooke's atom.

<sup>22</sup> We observe a crossing of potentials at  $r$ 's larger than shown in Fig. 2 also for the Helium atom. In this case, though, we cannot exclude it to be an artifact of the calculations. The exact potential in the case of Helium tends to 0 and this requirement added to a large- $r$  crossing would imply that the i-LDA potential should have two additional flexes. This seems to strongly affect the precision

of the calculations beyond the range shown.

<sup>23</sup> P. Mori-Sánchez, A. J. Cohen and W. Yang, *J. Chem. Phys.* **125**, 201102 (2006).

<sup>24</sup> A. Ruzsinszky, J.P. Perdew, G.I. Csonka, O.A. Vydrov, and G.E. Scuseria, *J. Chem. Phys.* **125**, 194112 (2006); *ibid* **126**, 104102 (2007).